

Kernel density estimation of a multidimensional efficiency profile

Anton Poluektov^{a,b}

^a*University of Warwick,*

Gibbet Hill Road, Coventry, CV4 7AL, UK

^a*Budker Institute of Nuclear Physics,*

630090, Lavrentieva 11, Novosibirsk, Russia

E-mail: Anton.Poluektov@cern.ch

ABSTRACT: Kernel density estimation is a convenient way to estimate the probability density of a distribution given the sample of data points. However, it has certain drawbacks: proper description of the density using narrow kernels needs large data samples, whereas if the kernel width is large, boundaries and narrow structures tend to be smeared. Here, an approach to correct for such effects, is proposed that uses an approximate density to describe narrow structures and boundaries. The approach is shown to be well suited for the description of the efficiency shape over a multidimensional phase space in a typical particle physics analysis. An example is given for the five-dimensional phase space of the $\Lambda_b^0 \rightarrow D^0 p \pi^-$ decay.

Contents

1. Introduction	1
2. Kernel density estimation basics	2
3. Boundary correction with approximation PDF	3
4. Practical considerations	5
5. Meerkat package	6
6. Application to $\Lambda_b^0 \rightarrow D^0 p \pi^-$ phase space	8
6.1 Estimation of the Dalitz plot density	9
6.2 Estimation of the angular density	11
6.3 Estimation of the full 5D density	12
7. Conclusion	13

1. Introduction

A common task in particle physics analyses (as well as in many other areas) is to obtain a functional representation of the probability density function (PDF) $p(x)$ for a vector of variables x from a data sample represented by a random set of values x_i . If the model behind the random process is known, a parametrised shape with a limited set of parameters is a good choice. This is, however, not always the case. Often the model is not known or is too complex (or simply is not a subject of the study), in which case finding a good parametrisation can be difficult. Using a simplified parametrisation leads to systematic biases, which have to be evaluated using alternative models. In the case of a multidimensional distribution, controlling the quality of a parametric fit can be difficult due to non-trivial correlations between the variables.

On the other hand, non-parametric approaches, such as spline interpolation or kernel density estimation do not require knowledge of the physics model behind the process and ensure the good quality of the PDF description by construction. These approaches, however, have their own shortcomings.

This paper discusses the application of the kernel density estimation (KDE) technique for the description of a multidimensional PDF. Typical problems related to the use of traditional KDE are discussed: correction of boundary effects and description of narrow structures. A modification of the KDE procedure is proposed to solve these problems, which is shown to work well in a typical use case of high-energy physics analysis. A real-life example of the description of the reconstruction efficiency in the five-dimensional phase space of the $\Lambda_b^0 \rightarrow D^0 p \pi^-$ decay is given. A software package which implements the proposed technique is described.

2. Kernel density estimation basics

Let us assume a random process which is characterised by a vector of variables x . The vector x is in general multidimensional, but we will give an example with a scalar variable first. The distribution of variable x follows a true PDF $P_{\text{true}}(x)$ that we need to estimate. Let x_i ($i = 1 \dots N$) be the data set which is sampled from this PDF. The kernel density estimator of the true PDF [1, 2] is

$$P_{\text{KDE}}(x) = \frac{1}{N} \sum_{i=1}^N K(x - x_i). \quad (2.1)$$

Here $K(x)$ is a kernel which is normalised to unity ($\int K(x)dx = 1$). Various alternative forms can be used for $K(x)$. The notable property of the KDE technique is that the quality of the PDF description depends rather weakly on the actual kernel used. In the following, we will use Epanechnikov [3] form:

$$K(x) = \begin{cases} \frac{3}{4\sigma} \left(1 - \frac{x^2}{\sigma^2}\right) & \text{for } x \in (-\sigma, \sigma) \\ 0 & \text{otherwise.} \end{cases} \quad (2.2)$$

This kernel is optimal in some sense (it optimises a certain figure of merit called the *asymptotic mean integrated square error*, *AMISE* [4]) and is easy to calculate.

Note that the resulting $P_{\text{KDE}}(x)$ in the limit $N \rightarrow \infty$ with the fixed kernel width σ is a convolution of the true PDF $P_{\text{true}}(x)$ with the kernel $K(x)$. Thus, if the true PDF has relatively narrow structures (with characteristic width smaller than or equal to the kernel width), they will be smeared. Certainly, with larger samples, the kernel can be made narrower, so that asymptotically the estimated PDF $P_{\text{KDE}}(x)$ will match the true one. For the limited sample size, however, one has to find a balance between the smearing of the PDF with large kernel widths, and the fluctuations of the estimated PDF with narrower kernels.

A typical problem of the KDE method is boundary effects. Direct use of Eq. (2.1) with a constant kernel results in an estimated PDF $P_{\text{KDE}}(x)$ that falls off at the edges of the distribution (Fig. 1). If the function is defined for $x > 0$ and is approximated by the linear function $1 + \alpha x$ near the boundary $x = 0$, the kernel PDF (2.1) will give, up to the terms linear in x ,

$$(1 + \alpha x)\theta(x) \otimes K(x) = \int_0^{\sigma-x} (1 + \alpha y) \frac{3}{4\sigma} \left(1 - \frac{y^2}{\sigma^2}\right) dy \simeq \left(\frac{1}{2} + \frac{3\alpha\sigma}{16}\right) + \left(\frac{\alpha}{2} + \frac{3}{4\sigma}\right)x, \quad (2.3)$$

where $\theta(x)$ is the threshold function that represents the boundary at $x = 0$:

$$\theta(x) = \begin{cases} 1 & \text{for } x \geq 0, \\ 0 & \text{for } x < 0. \end{cases} \quad (2.4)$$

Thus, if the kernel width is small compared to the inverse derivative of the true PDF, $1/\alpha$, KDE gives a value which is twice lower at the boundary than the true PDF. The boundary effect is demonstrated for the one-dimensional case in Fig. 1 for a uniform PDF, linear PDF, and the sum of a linear and a Gaussian PDF defined in the range $x \in (0, 1)$.

Numerous methods have been proposed to correct for boundary effects: data reflection [5], pseudodata [6, 7], kernel modification near the boundary [8, 9], transformation of variables [10].

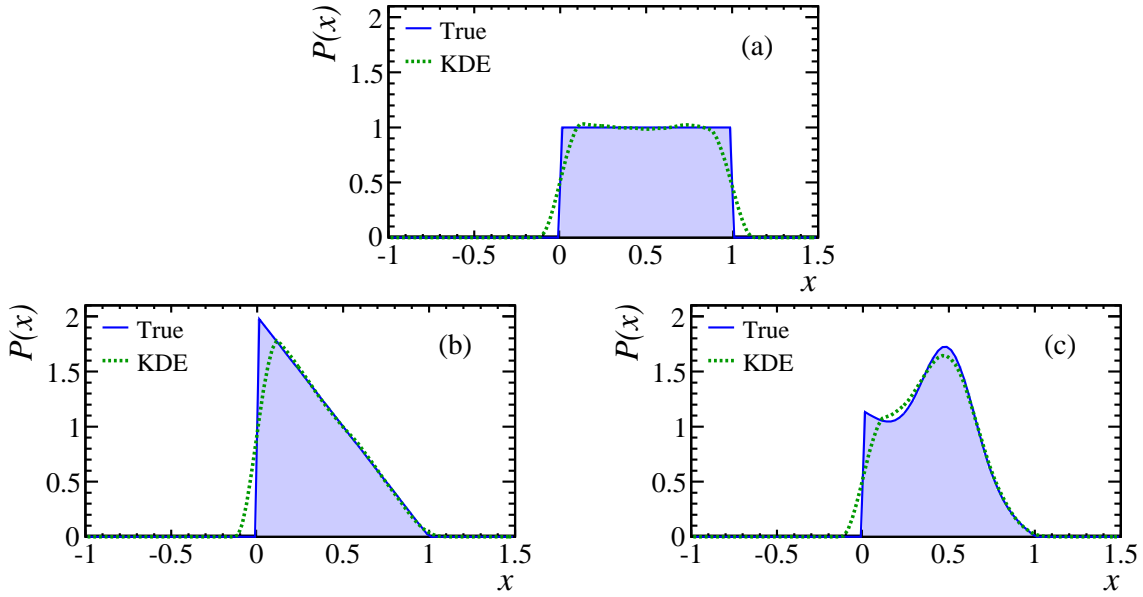


Figure 1. True PDF (filled area, blue solid line) and the result of kernel density estimation (red dashed line), corresponding to (a) uniform distribution, (b) linear distribution, and (c) sum of a linear and a Gaussian distributions.

In some particular cases, such as in the case of a periodic function, the boundary correction can be performed in an exact way; since we consider a general case here, these techniques are not discussed. Normally the methods listed above work well with simple boundaries, such as in the one-dimensional case, or in a multidimensional case with rectangular boundaries. It is not straightforward to apply these methods in the cases of complex boundaries, such as for conventional Dalitz plots [11].

3. Boundary correction with approximation PDF

A simple procedure is proposed here to correct for boundary effects, which works best if the approximate behaviour of the estimated function near the boundary is known. The procedure is illustrated below in a one-dimensional case, however it can also be applied in multiple dimensions with complex boundaries, as we will see later.

Let us first consider the function $P_{\text{corr}}(x)$ which is the ratio of the kernel PDF and the uniform function in the allowed region of x values convolved with the kernel¹:

$$P_{\text{corr}}(x) = \begin{cases} \frac{\sum_{i=1}^N K(x-x_i)}{(U \otimes K)(x)} & \text{for } x \in X, \\ 0 & \text{otherwise.} \end{cases} \quad (3.1)$$

The function $U(x)$ is the constant function in the allowed range of x and equals zero outside it:

$$U(x) = \begin{cases} 1 & \text{for } x \in X, \\ 0 & \text{otherwise.} \end{cases} \quad (3.2)$$

¹Here and below the normalisation of the PDF is arbitrary.

We can show how the PDF estimate of this form corrects for the boundary effect in the case of the linear PDF defined for $x > 0$ near the boundary. Similarly to Eq. (2.3), in the limit $N \rightarrow \infty$ we obtain

$$P_{\text{corr}}(x) = \frac{(1 + \alpha x)\theta(x) \otimes K(x)}{\theta(x) \otimes K(x)} = \frac{\int_0^{\sigma-x} (1 + \alpha y) \frac{3}{4\sigma} \left(1 - \frac{y^2}{\sigma^2}\right) dy}{\int_0^{\sigma-x} \frac{3}{4\sigma} \left(1 - \frac{y^2}{\sigma^2}\right) dy} \simeq \left(1 + \frac{3\alpha\sigma}{8}\right) + \frac{7\alpha x}{16} \quad (3.3)$$

up to the terms linear in x and σ . Thus, the approach given by Eq. (3.1), unlike the uncorrected KDE, is asymptotically unbiased at the boundary for small kernel widths ($\alpha\sigma \ll 1$). However, if the kernel width is large ($\alpha\sigma \sim 1$), as it is likely to be in the case of a multidimensional PDF, bias does occur.

The effect here is similar to that observed when the data reflection technique is used for boundary correction. In both cases, the kernel estimate is unbiased for small kernel widths, but the derivative of the estimated PDF at the boundary is underestimated: it equals zero by construction for the data reflection technique, and equals $7\alpha/16$ in the case above (so the bias is strictly smaller than for the data reflection technique). The effect of the boundary correction using Eq. (3.1) is illustrated in Fig. 2(a) for the linear true PDF.

Note that if the true PDF is flat at the boundary (*i.e.* if $\alpha = 0$), expression (3.1) does not lead to a bias even for the finite kernel width. One can now modify this expression in such a way that the estimate be unbiased not only for $\alpha = 0$, but in general for any *a-priori* known behaviour of the true PDF near the boundary. Let us assume that the true PDF is described by the approximation function $F(x)$ in the vicinity of the boundary ($x < \sigma$). Consider the expression of the form

$$P_{\text{approx}}(x) = \frac{\sum_{i=1}^N K(x - x_i)}{(F \otimes K)(x)} \times F(x). \quad (3.4)$$

In the limit of a large data sample ($N \rightarrow \infty$), for a fixed kernel width σ this expression is equal to the approximation PDF $F(x)$ near the boundaries, since $\sum_{i=1}^N K(x - x_i) \simeq (F \otimes K)(x)$. In the inner regions, where in the absence of narrow structures $(F \otimes K)(x) \simeq F(x)$, one obtains $P_{\text{approx}} \simeq P_{\text{KDE}}$. In the expression above we assume that the allowed region X of the values of variable x is defined by the function $F(x)$ such that $F(x) = 0$ for $x \notin X$.

As an example, we show the effect of PDF correction using Eq. (3.4) in Fig. 2(b). Here we estimate the PDF which is the sum of a linear and a Gaussian distributions, using the linear function as an approximation PDF.

The use of Eq. (3.4) is not only limited to the boundary correction. Other narrow structures, which otherwise would be smoothed out by the kernel, can also be described by the approximation PDF $F(x)$. In general, if the PDF we want to parametrise can be factorised as $P_{\text{true}}(x) = f(x)F(x)$, where $F(x)$ is a known function which possibly contains narrow structures, while $f(x)$ is slowly varying compared to the kernel width, it can be efficiently parametrised by this technique. In other words, the kernel density estimator in Eq. (3.4) describes the *relative* variations of the PDF with respect to the approximation function $F(x)$. We will therefore refer to this approach as the *relative kernel density estimation* technique.

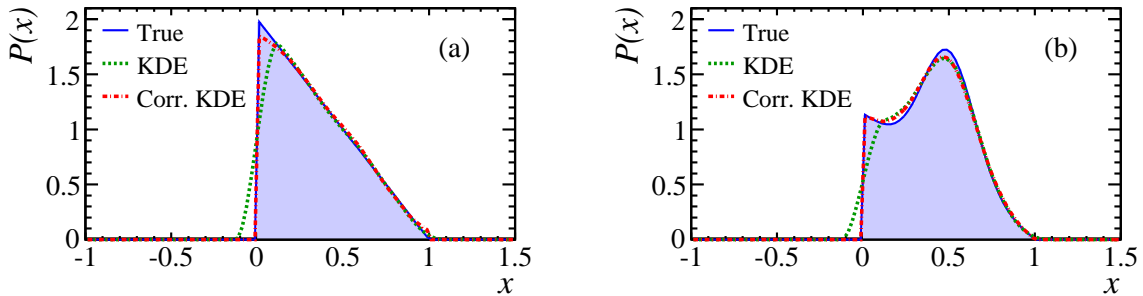


Figure 2. (a) True PDF (filled area, blue solid line), the result of kernel density estimation (green dashed line), and of the KDE corrected as in Eq. (3.1) (red dash-dotted line). (b) The same for the sum of a linear and a Gaussian distribution, with correction applied as in Eq. (3.4) using a linear PDF as an approximation.

The proposed approach where a nonparametric correction is applied on top of an approximation PDF can be effectively applied in many cases for multidimensional PDFs. In general, obtaining PDF estimation for a multidimensional function requires large data samples. Often, however, the PDF can be approximately factorised as a product of several PDFs with reduced number of dimensions. In the approximation approach, these PDFs can be described again using the same kernel density technique with a kernel of narrower width. The approximation PDF can then be taken as the product of these PDFs, while the residual correction can be applied using the proposed approach with a larger kernel width.

A typical particle physics analysis uses a description of the efficiency profile from full detector simulation which is an extremely CPU-consuming task. Using the proposed approach can help reduce the required simulation sample. For instance, an approximation efficiency function can be obtained from a large sample of data obtained using simplified, but fast simulation, while the final correction can come from the sample of full detector simulation.

4. Practical considerations

Direct usage of the relative KDE approach as in Eq. (3.4) in the fit of experimental data can in practice be slow. For each data point x one has to calculate the convolution of the approximation function $F(x)$ with the kernel. In general, if the convolution is not expressed analytically, one has to use Monte-Carlo (MC) integration or a similar numerical technique to calculate it. It could be more effective to store the calculated values of the estimated PDF on a multidimensional grid, and use linear interpolation between the grid nodes to calculate the values of the function in the data fit.

Calculation of the function using linear interpolation between the nodes of a rectangular grid in the presence of a (in general, curved) physical boundary, however, is not straightforward. To obtain the value of the function for points close to the boundary, the function has to be calculated for nodes which are outside of the boundary. Fortunately, the relative KDE approach allows extrapolation of the function $P(x)$ beyond the boundary under certain conditions: the density expressed by Eq. (3.4) can be calculated for the points beyond the boundary if the distance between the extrapolated point and the boundary is small compared to the kernel width.

Interpolation can be applied directly to the result of relative KDE estimation (3.4), *i.e.*

$$P_{\text{interp}}(x) = \text{Bin}(P_{\text{approx}}(x)) = \text{Bin} \left(\frac{\sum_{i=1}^N K(x-x_i)}{(F \otimes K)(x)} \times F(x) \right), \quad (4.1)$$

where the functor $\text{Bin}(f)$ denotes multilinear interpolation of the function f over the rectangular grid. However, calculating $P_{\text{interp}}(x)$ in this way is computationally intensive. For k grid points, a vector of data x_i of size n and N points in the toy MC convolution vector, the calculation takes time proportional to $k(n+N)$, and needs both the data vector and convolution vector to be kept in memory. An alternative approach is to perform linear interpolation for both the numerator and denominator of Eq. (3.4):

$$P_{\text{interp}}(x) = \frac{\text{Bin} \left(\sum_{i=1}^N K(x-x_i) \right)}{\text{Bin}((F \otimes K)(x))} \times F(x). \quad (4.2)$$

In that case one has to loop through the data and convolution vectors only once, and thus they don't need to be kept in memory. In addition, for each point of the data vector, one has to loop through not all the nodes of the grid, but only over those nodes which are less than a kernel width apart from the point x_i .

None of the expressions above assume that the kernel is constant over the phase space. It is therefore possible to apply an adaptive kernel technique, where the kernel width is a function of the PDF value. In practice, this would result in an iterative procedure, where the kernel width in each iteration depends on the PDF value calculated in the previous iteration. Such an approach could be useful for PDFs containing sharp peaks.

The conventional kernel density estimator works naturally with weighted data sets, where each event x_i has its individual weight w_i . In that case, Eq. (2.1) becomes

$$P_{\text{KDE}}(x) = \frac{\sum_{i=1}^N w_i K(x-x_i)}{\sum_{i=1}^N w_i}. \quad (4.3)$$

The relative KDE technique is also easily generalised to deal with weighted data sets in a similar way, by using the weighted sum in the numerator of Eq. (3.4).

5. Meerkat package

The technique described here has been implemented in the software package called Meerkat (which stands for ‘‘Multidimensional Efficiency Estimation using the Relative Kernel Approximation Technique’’), available at HepForge [12]. The package provides a set of C++ classes for the estimation of a PDF of any (reasonable) dimensionality defined over a phase space which is the combination of Dalitz plot phase spaces, one-dimensional phase spaces, and phase spaces with limits defined in a functional form. The code depends on the ROOT [13] framework.

The classes of the Meerkat library are derived from one of two abstract classes, `AbsPhaseSpace` which describes the phase space, and `AbsDensity` which defines the interface for the PDF classes. The classes derived from `AbsPhaseSpace` are as follows:

- `OneDimPhaseSpace` describes a one-dimensional phase space, which is just the finite range of values of the single scalar variable.
- `DalitzPhaseSpace` is the two-dimensional phase space of the Dalitz plot, the kinematic phase space of the decay of a particle into three other particles.
- `ParametricPhaseSpace` allows to define an arbitrary phase space where the boundaries (lower and upper limit) of one variable are functions of variables over another phase space.
- `CombinedPhaseSpace` describes a combination (direct product) of several component phase spaces.

The classes derived from `AbsDensity` are:

- `UniformDensity` is a uniform density over arbitrary phase space.
- `FormulaDensity` represents a fixed density which is defined in a functional form. Both `UniformDensity` and `FormulaDensity` can be used as the approximation PDFs for the kernel density estimator.
- `KernelDensity` implements the unbinned relative KDE procedure defined by Eq. (3.4).
- `BinnedDensity` defines a PDF which is the result of multilinear interpolation of a PDF over arbitrary phase space (*i.e.* it implements the $Bin(f)$ functor as in Eq. (4.1)).
- `BinnedKernelDensity` implements the binned approach as in Eq. (4.2). It is much more efficient from the point of view of computational time and memory usage than `KernelDensity`, and is thus recommended, except for the special cases when the binning introduces unacceptable distortions of the approximation function.
- `AdaptiveKernelDensity` implements the same approach as `BinnedKernelDensity`, but with a variable kernel width which is a function of the value of another PDF (*e.g.* of the PDF estimated at the previous iteration). Both `BinnedKernelDensity` and `AdaptiveKernelDensity` classes can work with weighted data sets.
- `FactorisedDensity` is the density which is simply a product of two or more densities of different (sets of) variables. `FactorisedDensity` can, for instance, be used as approximation PDF for `BinnedKernelDensity`.

The code also contains several examples of usage of these classes.

6. Application to $\Lambda_b^0 \rightarrow D^0 p \pi^-$ phase space

One possible use case of the procedure proposed here is the description of efficiency, background, and similar quantities over multidimensional kinematic phase space in high-energy physics processes.² In a multidimensional case, the size of the data sample to be used to parametrise these quantities becomes a critical issue. It is often assumed that some or all the kinematic variables describing the decay are uncorrelated and thus the PDF can be represented in a factorised form. This effectively reduces the dimensionality and the size of the data sample needed. However, possible deviation from the factorisation assumption can bias the measurement and has to be treated as a systematic uncertainty. In cases when the correlations between the variables are small, or at least not changing rapidly, the approach proposed here can be efficiently used.

Below we illustrate this approach in the real-life application to the description of the selection efficiency of the baryonic decay $\Lambda_b^0 \rightarrow D^0 p \pi^-$ which is being studied at the LHCb experiment [14]. This is a three-body decay where both the initial and the final states contain spin-1/2 particles (Λ_b^0 and the proton). In the general case, the kinematic distribution is fully described by five variables. One can choose *e. g.*, two squared invariant masses of the pairs of final state particles, $M^2(D^0 p)$ and $M^2(p \pi)$, and three angles which describe the orientation of the decay plane in a certain reference frame, θ_p , ϕ_p and $\phi_{D\pi}$.

To validate the proposed procedure we need a large sample of decays, therefore we use a simplified simulation of the LHCb detector response. Our simulation reflects the forward geometry of the LHCb detector [15], which instruments the region close to the beam line of the LHC. We use coordinates where the z axis corresponds to the beam line, and the instrumented region is at $z > 0$. Decays of Λ_b^0 baryons are generated using the EvtGen [16] package with uniform distribution in the $D^0 p \pi$ phase space with D^0 decaying to $K^- \pi^+$. Λ_b^0 baryons are generated unpolarised, with uniform distribution in pseudorapidity $\eta = -\log \tan \theta/2$ in the range $1.5 < \eta < 5.5$ (where θ is the polar angle in the chosen frame), are distributed uniformly in azimuthal angle ϕ and have exponential distribution of the transverse (with respect to the beam line) momentum

$$f(p_T) \propto \exp(-p_T/p_T^0), \quad (6.1)$$

where $p_T^0 = 5 \text{ GeV}/c$. To simulate the tracking system and trigger response and the offline selection, the following requirements are applied to the decay products of the Λ_b^0 :

- All charged particles in the final state are required to have pseudorapidity in the range $2 < \eta < 5$ (tracking system acceptance), transverse momentum $p_T > 0.15 \text{ GeV}/c$ (offline selection to reduce background) and momentum $p < 100 \text{ GeV}/c$ (requirement of reliable particle identification).
- Pions and kaons in the final state have to satisfy $p > 5 \text{ GeV}/c$, while protons are required to have $p > 10 \text{ GeV}/c$ (particle identification thresholds).

²In the following, we will refer to all these quantities as “probability densities” while, strictly speaking, these functions are only proportional to the PDFs estimated from the samples of random points. In our task of estimating the multidimensional shape of these functions, correcting the common normalisation is straightforward and is thus not discussed.

- At least one particle in the final state is required to have transverse momentum $p_T > 3.5$ GeV/ c (hardware trigger selection).

In this example we will illustrate the strong point of the proposed approach that is the possibility to gradually, in several steps, increase the dimensionality of the PDF estimator, by using the factorised approximation PDF from the previous step, and correcting for correlations using the relative KDE technique.

We will see how well the 5D distribution of the $\Lambda_b^0 \rightarrow D^0 p \pi^-$ decay can be estimated using a sample of limited size of 10^5 decays. We make use of a large sample of simulated data (10^8 events) to obtain the reference (“true”) distribution of the efficiency with a relatively narrow kernel, and then use subsamples of 10^5 events to evaluate the quality of the PDF estimation in comparison with the reference PDF. The kernel width for the KDE with a limited data sample has to be optimised to reach a balance between the statistical fluctuations of the estimated PDF (which increase for narrower widths) and systematic bias due to smearing of the structures (which becomes critical for wider kernels). The following figure of merit is used to evaluate the quality of the estimation:

$$Q = \sqrt{\sigma^2 + \Delta^2}, \quad (6.2)$$

where

$$\sigma = \langle RMS_i(F_i(x_\alpha)) \rangle_\alpha \quad (6.3)$$

is the variance σ_α of the PDF values in the node α of the rectangular grid, averaged over all nodes within the allowed phase space, and

$$\Delta = RMS_\alpha(\langle F_i(x_\alpha) \rangle_i) \quad (6.4)$$

is the RMS (calculated over the nodes α of the rectangular grid) of the average bias of estimated PDF values with respect to the reference value. Here $\langle \dots \rangle_i$ and $\langle \dots \rangle_\alpha$ denote averaging over the subsample and grid node, respectively, while $RMS_i(\dots)$ and $RMS_\alpha(\dots)$ mean taking the RMS value.

6.1 Estimation of the Dalitz plot density

Before we start to deal with the full 5D phase space, we will consider the estimation of PDFs with reduced dimensionality. These PDFs will then be used as components of the 5D approximation PDF. We start with the estimation of the 2D distribution in Dalitz plot variables $M^2(D^0 p)$ and $M^2(p\pi)$. The characteristic property of this distribution is that the allowed phase space in these variables has a non-trivial shape, with the range of one variable depending on the value of the other.

Reference density over the Dalitz plot, obtained with a narrow kernel of $0.3 \text{ GeV}^2/c^4$ width in both $M^2(D^0 p)$ and $M^2(p\pi)$ variables from the sample of 10^8 simulated decays, is shown in Fig. 3 (a). Figure 3 (b) shows an example of the density obtained from a sample of 10^5 events with a kernel width of $1.5 \text{ GeV}^2/c^4$. To allow direct comparison, all PDFs are normalised such that the average PDF value over the phase space equals to one. As a result of running the PDF estimation on 50 samples of 10^5 events, we find the bias and variance of the PDF value as a function of Dalitz plot position. These are shown in Figs. 3 (c) and (d), respectively. The quantities Δ and σ are

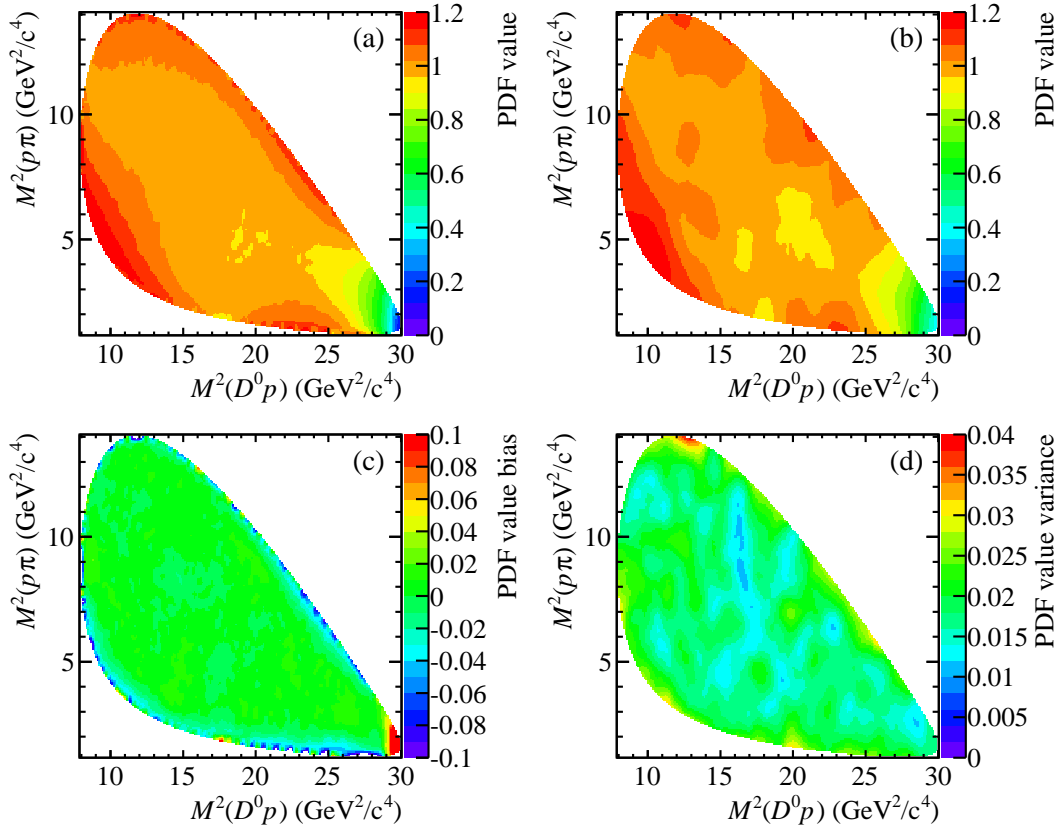


Figure 3. Results of the estimation of the efficiency of $\Lambda_b^0 \rightarrow D^0 p \pi^-$ decays across the Dalitz plot. (a) Reference density obtained with narrow kernel and (b) an example of density obtained with 10^5 sample size and kernel width of $2 \text{ GeV}^2/c^4$. (c) Average bias and (d) variance of estimated PDF values as a function of Dalitz plot position.

Table 1. Results of the estimation of the Dalitz plot efficiency profile for the $\Lambda_b^0 \rightarrow D^0 p \pi^-$ decays. Systematic (Δ), variance (σ) terms and the overall figure of merit Q are given for different kernel widths.

Kernel width, MeV^2/c^4	Bias Δ	Variance σ	Q
1.0	0.0084	0.0159	0.0179
1.5	0.0125	0.0107	0.0165
2.0	0.0173	0.0081	0.0191

calculated from these distributions. The values of RMS bias Δ and average variance σ , as well as the overall quality of the density estimation Q , are given in Table 1 for three different kernel widths. The width of $1.5 \text{ GeV}^2/c^4$ gives the best value of $Q = 0.0165$. This can be interpreted as that the average precision of the PDF value estimation (including statistical and systematic effects) is 1.65%.

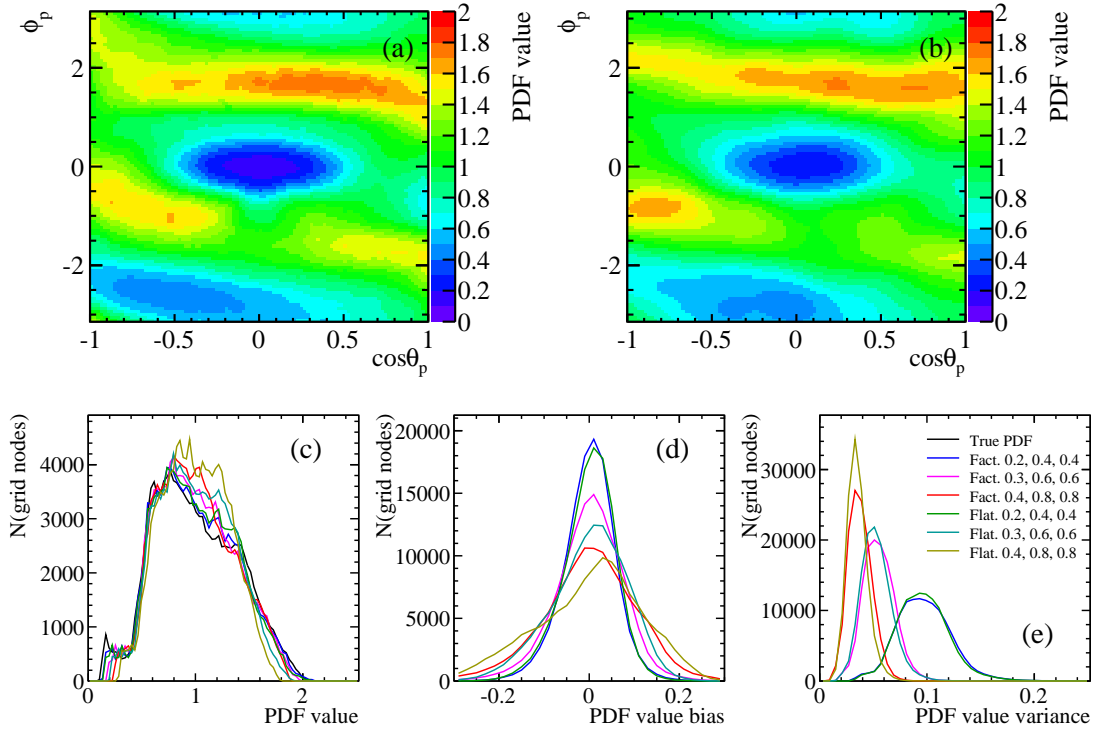


Figure 4. Results of the estimation of the efficiency of $\Lambda_b^0 \rightarrow D^0 p \pi^-$ decays in angular variables. (a) Slice of reference density obtained with narrow kernel and (b) an example of the same slice obtained with 10^5 sample size and kernel widths of (0.3, 0.6, 0.6). (c) Distribution of PDF values, and distributions of (d) average bias and (e) variance of estimated PDF values.

6.2 Estimation of the angular density

The second component of the $\Lambda_b^0 \rightarrow D^0 p \pi^-$ phase space is the angular part, which is described by three angles. The variables used to describe it are defined in the rest frame of the decaying Λ_b^0 , with the x' axis given by its direction in the laboratory frame, the polarisation axis z' given by the cross product of the beam and x' axes, and the y' axis by the cross product of the z' and x' axes. The three variables are cosine $\cos \theta_p$ of the polar angle and the azimuthal angle ϕ_p of the proton momentum in this reference frame, and the angle ϕ_{Dp} between the $D^0 \pi$ -plane and the plane formed by the proton and polarisation axis.

As above, we use the large sample with narrow kernel to obtain the reference PDF. Since the phase space is now three-dimensional, we can only plot its slice in a pair of variables. As an example, the slice in $(\cos \theta_p, \phi_p)$ plane for $\phi_{Dp} = \pi/4$ is shown in Fig. 4 (a). Figure 4 (b) shows the same slice for a sample of 10^5 events and the kernel widths of (0.3, 0.6 rad, 0.6 rad) in the three variables.

Instead of presenting the bias and variance of the PDF values as a function of phase space position, as we did for the Dalitz plot distribution, we now show the distributions of these values over the points across the phase space in the form of histograms. Figures 4 (c), (d) and (e) show histograms of the PDF value, its bias with respect to the reference density, and variance, respectively, where each entry corresponds to a node of the rectangular grid in the three-dimensional angular

Table 2. Results of the estimation of the angular efficiency of $\Lambda_b^0 \rightarrow D^0 p \pi^-$ decays. Systematic (Δ), variance (σ) terms and the overall figure of merit Q for different kernel widths and flat and factorised approximation PDFs.

Kernel width	Appr. PDF	Bias Δ	Variance σ	Q
0.2, 0.4, 0.4	Flat	0.059	0.097	0.113
0.3, 0.6, 0.6	Flat	0.085	0.053	0.100
0.4, 0.8, 0.8	Flat	0.117	0.035	0.122
0.2, 0.4, 0.4	Factorised	0.058	0.097	0.113
0.3, 0.6, 0.6	Factorised	0.076	0.055	0.094
0.4, 0.8, 0.8	Factorised	0.106	0.038	0.113

phase space. The value of Δ is thus the RMS of the distribution in Fig. 4 (d), and the value of σ is the mean of the distribution in Fig. 4 (e).

We test two different options for the approximation PDF used to estimate the angular density. We compare results with the uniform approximation PDF (“flat” approximation), and an approximation PDF which is the product of distributions in each of the angles (“factorised” approximation). For the latter, the density for each individual variable is in turn the result of applying the relative KDE method with the uniform approximation PDF. Results for these two approaches with different kernel widths are summarised in Table 2. The factorised approximation PDF gives a better quality.

6.3 Estimation of the full 5D density

The full 5D density of the decay $\Lambda_b^0 \rightarrow D^0 p \pi^-$ is estimated with several different approaches. First, we test the factorised PDF which is the product of Dalitz and angular densities. We also try 5D relative KDE estimators with different approximation PDFs: uniform (“flat”), factorised PDF made of Dalitz and angular densities (“2D×3D”), as well as factorised PDF which is a product of Dalitz density and densities of each of the three angular variables (“2D×(1D)³”). The kernel widths for the components of the factorised PDFs are taken to be those that optimise the Q value in Sections. 6.1 and 6.2. For the full 5D kernel, we use the width which is larger by a factor s than the kernel width of the component densities.

The results of the 5D PDF estimation are given in Fig. 5. Figure 5 (a) and (b) show the Dalitz plot and $(\cos \theta_p, \phi_p)$ slices of the reference PDF which is obtained as explained above. The same slices for the PDF estimated using 10^5 sample with the relative KDE method and 2D×3D approximation PDF are shown in Fig. 5 (c) and (d). This estimation uses a width factor $s = 2$ for the 5D kernel. Figures 5 (e), (f), and (g) show the distributions of PDF value, PDF bias and its variance, respectively, as in Section 6.2.

The quantitative results of the estimation are given in Table 3. As can be seen from the table, the best approach using relative KDE technique (which uses 2D×3D approximation PDF) gives on average twice lower figure of merit ($Q = 0.178$) of PDF estimation than the product of Dalitz and angular densities ($Q = 0.353$).

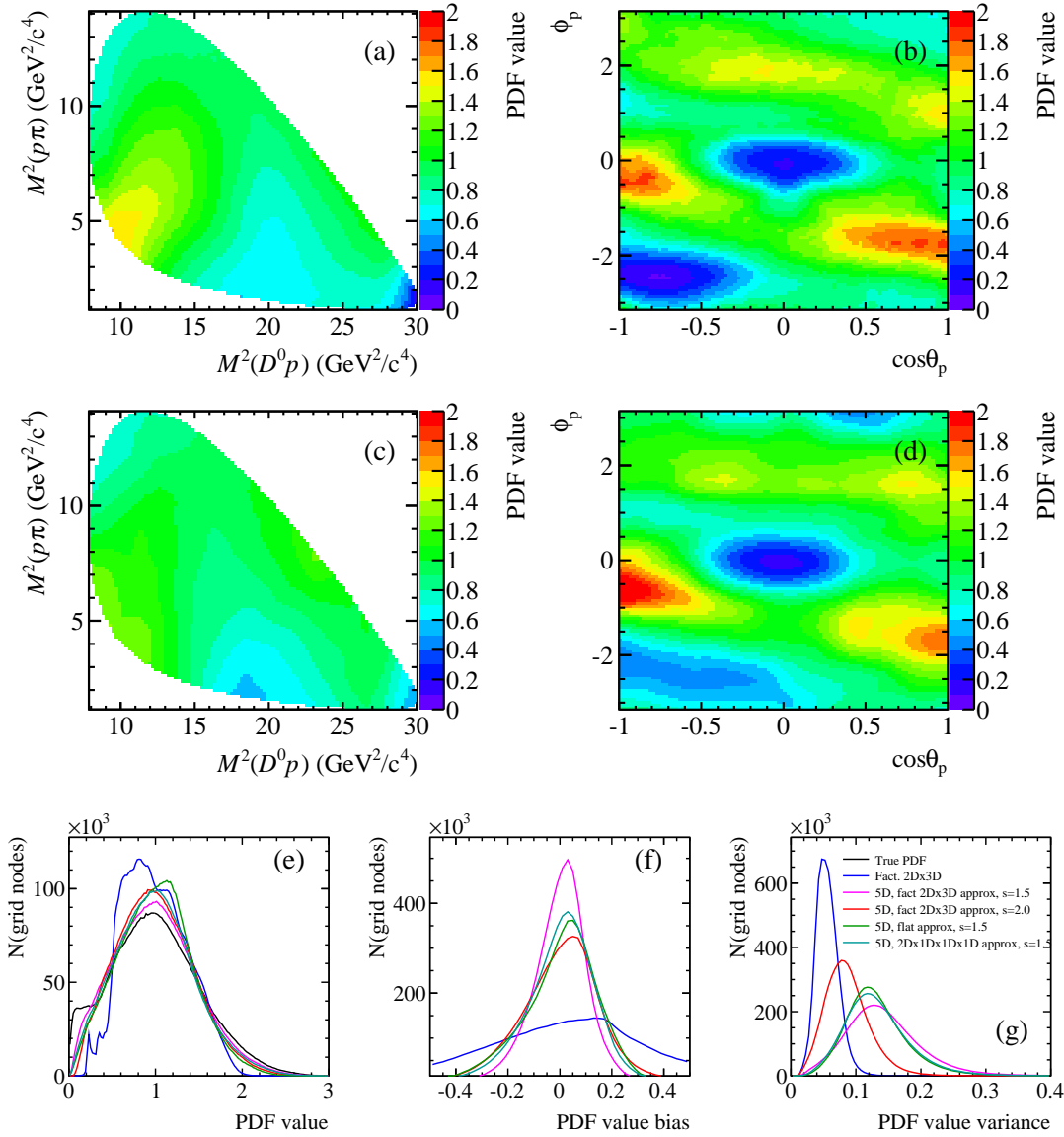


Figure 5. Results of the estimation of the 5D efficiency of $\Lambda_b^0 \rightarrow D^0 p \pi^-$ decays. Slice of reference density obtained with narrow kernel in (a) Dalitz plot and (b) angular variables, and (c,d) an example of the same slices obtained with 10^5 sample size and kernel widths of $(1.5 \text{ GeV}^2/c^4, 1.5 \text{ GeV}^2/c^4, 0.25, 0.5, 0.5)$. (e) Distribution of PDF values, and distributions of (f) average bias and (g) variance of estimated PDF values.

7. Conclusion

A simple modification of the kernel density estimation technique is proposed to correct for boundary effects and other expected narrow (with respect to the kernel width) structures. In this approach, the estimated PDF is represented as the product of the approximated PDF, which describes the behaviour near the boundaries and narrow structures, and the kernel density PDF.

This approach is shown to work well in the case of description of the five-dimensional efficiency shape for the decay $\Lambda_b^0 \rightarrow D^0 p \pi^-$. Approximation PDF is the factorised PDF of the phase

Table 3. Results of the estimation of the 5D efficiency of $\Lambda_b^0 \rightarrow D^0 p \pi^-$ decays. Systematic (Δ), variance (σ) terms and the overall figure of merit Q for different approaches.

Kernel width factor s	PDF	Bias Δ	Variance σ	Q
-	2D \times 3D factorised	0.349	0.056	0.353
2.0	5D, fact. 2D \times 3D approx.	0.159	0.087	0.181
1.5	5D, fact. 2D \times 3D approx.	0.108	0.142	0.178
1.5	5D, flat approximation	0.150	0.132	0.200
1.5	5D, fact. 2D \times (1D) ³ approx.	0.140	0.132	0.192

space variables, while the relative KDE provides a smooth correction to take into account the correlations between the phase space variables. This allows to use a relatively wide kernel for the multidimensional PDF estimation which reduces fluctuations due to limited sample size, while still keeping the essential features of the PDF (*e.g.* near the boundaries of the phase space) not smeared by the kernel.

Acknowledgments

The author is grateful to his colleagues from the LHCb collaboration for useful discussions about the method, feedback on the usage of `MeerKat` package, and suggestions to improve the text of the paper: Thomas Blake, Tim Gershon, Michal Kreps, Thomas Latham, Mark Whitehead (University of Warwick), Michael Williams (MIT), Peter Griffith (University of Birmingham).

This work is supported by the Science and Technology Facilities Council (United Kingdom), by the Russian Foundation for Basic Research grant 14-02-00569 A, and by the Russian Ministry of Education and Science contract 14.610.21.0002.

References

- [1] M. Rosenblatt, *Remarks on some nonparametric estimates of a density function*, *Ann. Math. Statist.* **27** (1956) 569.
- [2] E. Parzen, *On estimation of a probability density function and mode*, *Ann. Math. Statist.* **33** (1962) 847.
- [3] V. A. Epanechnikov, *Non-parametric estimation of a multivariate probability density*, *Theory Probab. Appl.* **14** (1969) 153–158.
- [4] J. L. Hodges and E. L. Lehmann, *The efficiency of some nonparametric competitors to the t-test*, *Annal of Mathematical Statistics* **13** (1956) 324.
- [5] E. Schuster, *Incorporating support constraints into nonparametric estimators of densities*, *Communications in Statistics, Part A - Theory and Methods* **14** (1958) 1123.
- [6] A. Cowling and P. Hall, *On pseudodata methods for removing boundary effects in kernel density estimation.*, *J. Roy. Statist. Soc. Ser. B* **58** (1996) 551.

- [7] P. Hall and T. E. Wehrly, *A geometrical method for removing edge effects from kernel-type nonparametric regression estimators*, *Journal of the American Statistical Association* **86** (1991) 665.
- [8] M. Jones, *Simple boundary correction for kernel density estimation.*, *Statistics and Computing* **3** (1993) 135.
- [9] M. Jones and P. Foster, *A simple nonnegative boundary correction method for kernel density estimation*, *Statistica Sinica* **6** (1996) 1005.
- [10] M. P. Wand, J. S. Marron, and D. Ruppert, *Transformations in density estimation (with comments)*, *Journal of the American Statistical Association* **86** (1991) 343.
- [11] R. H. Dalitz, *On the analysis of τ -meson data and the nature of the τ -meson*, *Philosophical Magazine* **44** (1953) 1068.
- [12] <http://meerkat.hepforge.org>
- [13] R. Brun and F. Rademakers, *Root — an object oriented data analysis framework*, *Nucl. Instrum. Meth.* **A389** (1997) 81–86.
- [14] LHCb Collaboration, R. Aaij et al., *Studies of beauty baryon decays to $D^0 p h^-$ and $\Lambda_c^+ h^-$ final states*, *Phys.Rev.* **D89** (2014), 032001.
- [15] LHCb collaboration, A. A. Alves Jr. et al., *The LHCb detector at the LHC*, *JINST* **3** (2008) S08005.
- [16] D. J. Lange, *The EvtGen particle decay simulation package*, *Nucl. Instrum. Meth.* **A462** (2001) 152–155.